Delay-Aware Rate Control for Multi-User Scalable Video Streaming Over Mobile Wireless Networks

Hassan Mansour, Vikram Krishnamurthy, and Panos Nasiopoulos
Department of Electrical and Computer Engineering
University of British Columbia
Email: {hassanm, vikramk, panos}@ece.ubc.ca

***Abstract*—In this paper, we propose a delay and capacity constrained multi-user scalable video streaming scheme that improves the average end-to-end distortion of transmitted video streams compared to traditional streaming strategies. Wireless video streaming applications are characterized by their bandwidth-intensity, delay-sensitivity, and loss-tolerance. Our main contributions include: (i) an analytical expression for packet delay and play-out deadline of unequal erasure protection (UXP) protected scalable video, (ii) an analysis of the performance of delay-aware, capacity-aware rate allocation for optimized UXP streaming scenarios, (iii) proof that unequal error protection causes a rate-constrained optimization problem to be non-convex. Performance evaluations using a 3GPP network simulator show that, for different channel capacities and packet loss rates, delay-aware non-stationary rate-allocation delivers significant gains which range between 1.65dB to 2dB in average Y-PSNR of the received video streams over delay-unaware strategies. These gains come at a cost of increased *off-line* computation which is performed prior to the streaming session and therefore, do not affect the run-time performance of the streaming system.**

***Index Terms*—Wireless video streaming, SVC, UXP, streaming delay analysis.**

I. Introduction

The advances in wireless and mobile network technologies are enabling a multitude of multimedia streaming applications. These advances are triggering an accelerated growth in wireless video streaming applications that are bandwidth-intense, delay-sensitive, and loss-tolerant [1]. Broadband ad hoc wireless networks and high-throughput mobile 3G networks, such as IEEE 802.11-based wireless local area networks (WLAN) and high-speed downlink packet access (HSDPA) respectively, are being deployed at an expanding pace and the number of subscribers to video streaming services is on the increase [2]. However, with the expanding availability of streaming services comes the demand for streaming and scheduling policies that manage the large data volume.

A typical video streaming system, as described by Chou et. al. [3], can be separated into three major components: a streaming server that stores pre-encoded video data, a communication channel over which the encoded video data is transmitted, and several clients with receiver buffers that can store up to a few seconds of received data and then begin playback until the end of the streaming session. Several streaming scenarios can be handled by the aforementioned streaming system. We will address the case of streaming scalable video data to multiple users over a wireless channel that suffers from packet loss, variable delivery delay, and limited capacity.

A. Main Results

In this paper, we propose a delay and capacity constrained multi-user scalable video streaming scenario and analyze its performance compared to several media-aware scalable video streaming scenarios over lossy channels. The main contributions of this paper are summarized as follows:

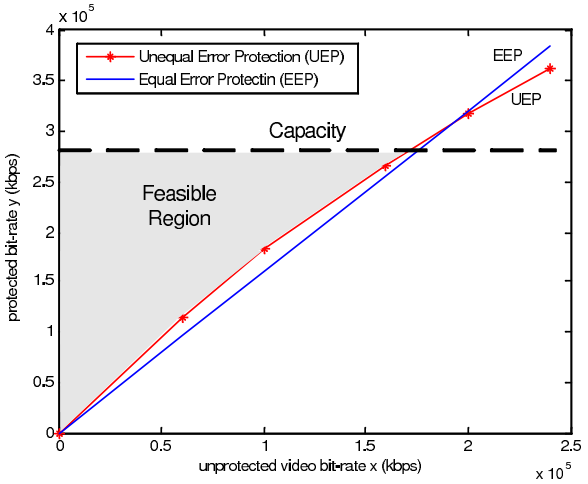

Fig. 1. The plot shows that unequal error protection (UEP) results naturally in a non-convex optimization problem as witnessed by the concavity of the UEP function compared to linearity of equal error protection (EEP). The protected bit-rate region is bounded by the available channel capacity.

1) We derive an analytical expression for packet delay and play-out deadline of unequal erasure protection (UXP) protected scalable video. A group of coded video frames (GOP) is embedded in a single UXP transmission block (TB) thus changing the play-out deadline of the protected packets. Therefore, we derive an upper bound for the number of link-layer (RLC) frames allowed per TB as a function of the RLC frame delivery delay.
2) We analyze the performance of delay-aware, capacity-aware, and rate-minimized UXP in conjunction with optimized rate-allocation compared to simpler streaming strategies.
3) We analyze the properties of the rate-constrained optimization problem in terms of convexity and complexity.

Our preliminary observations indicate that using unequal error protection renders any optimization problem with bit-rate constraint as non-convex since the bit-rate constraint equation is piecewise concave as illustrated in Figure 1.

B. Literature Review

Extensive research has been done in this field starting with the pioneering work of Chou et. al. [3] in which the problem of rate-distortion optimized (RaDiO) streaming of an entire video presentation is reduced to the problem of error-cost optimized transmission of an isolated data unit. To our knowledge, the most closely related work is that in [2] and [4]. In [2], Pahlawatta et. al. investigate channel-aware resource allocation and packet scheduling for the transmission of scalable video over wireless networks such as HSDPA and IEEE 802.16. However, no application layer FEC or delay analysis are considered, which are major components of the work presented in this paper. The work in [4] considers the problem of rate allocation for multiple streaming sessions sharing multiple access networks. An analytical framework is developed for optimal video rate allocation, based on observed available bit rate and round trip time over each access network, as well as the video distortion-rate characteristics. However, we present a rate-distortion model that includes the effect of application layer UXP on the decoded video distortion and develop the corresponding delay analysis. Furthermore, *the main conclusions of the aforementioned works that we wish to draw upon are the importance of delay analysis and delay-aware rate control in multi-user video streaming.*

The remainder of this paper is organized as follows: we present in Section II the different components of a multi-user video streaming system in terms of multi-user rate allocation, unequal error protection. In Section III we present the packet delay analysis caused by the underlying architecture and limitations of the transmission channel. In Section IV we show that unequal error protection results in a non-convex rate-constrained optimization problem. The performance of the proposed media-aware multi-user video streaming algorithms are analyzed and discussed in Section V, and finally we present our conclusions in Section VI.

II. Multi-User Bit-rate Allocation with UXP Protection

In this section, we present the different components of a multi-user video streaming system in terms of video rate-distortion characteristics, and the underlying architecture and limitations of the transmission channel.

Figure 2 shows a streaming server that has access to U pre-encoded scalable video streams intended for delivery to U clients/users. The server receives channel quality information from the link/MAC layer in terms of radio link control (RLC) frame loss rate, estimated channel capacity, and estimated packet delivery delay.

A. UXP error protection

Several solutions have been proposed to combat packet losses in scalable coded media with an increasing inclination towards the use of application layer Forward Error Correction (FEC). Unequal Erasure Protection (UXP) is one example of FEC techniques that are being promoted for the protection of scalable video data from losses during transmission [5]. The effectiveness of UXP for the protection of scalable video has been demonstrated in [6]. UXP is a Forward Error Correction (FEC) scheme that is based on Reed-Solomon (RS) codes. Under UXP, video packets of a GOP are grouped together into a transmission block (TB).

Each row of a TB constitutes an (n, k) RS codeword, where n is the length of the codeword in bytes, k is the number of data bytes (coded video bytes), and $n-k$ bytes are parity bytes, where $\frac{n}{2} < k \leq n$. Each column of a TB is then encapsulated in an RTP packet, which enables UXP to correct up to $n-k$ packet erasures. In [6], different protection classes are defined for each FGS enhancement layer, higher layers receiving less protection than lower FGS layers and the base layer. Figure 3 illustrates the UXP scheme described above.

B. Video Rate-Distortion Models

Let $u \in \mathcal{U}$, where $\mathcal{U} = \{1, 2, ...U\}$, be the video/user index. Each FGS scalable video indexed by u is characterized by a bit-rate $r_u \in [L_u, H_u]$, where L_u is the base-layer bit-rate and H_u is the maximum video bit-rate which includes all enhancement layers. Let p be the RLC packet loss rate and N_{max} the maximum number of RLC retransmissions, we define the pair $\{R_u(r_u), D_u(r_u)\}$ as the protected video bit-rate and the total video distortion after channel loss, respectively, such that

$$\begin{aligned} R_u(r_u) &= (1+\gamma) R_{\mathrm{UXP}}(r_u) \\ &= \left(1 + \sum_{j=0}^{N_{max}} j(1-p)p^j\right) \int_{L_u}^{r_u} \frac{n}{k_u(x)} dx \\ D_u(r_u) &= D_{\mathrm{enc}}(r_u) + D_{\mathrm{loss}}(r_u) \\ &= \alpha_u + \frac{\theta_u}{r_u - \beta_u} + \int_{L_u}^{r_u} \left(\frac{\theta_u}{(x-\beta_u)^2}\right) P_u(x) dx \end{aligned} \quad (1)$$

where $\gamma = \sum_{j=0}^{N_{max}} j(1-p)p^j$ is the channel redundancy due to MAC retransmissions, $D_{enc}(r_u)$ is the video encoder distortion model used in [4] with parameters α_u, θ_u, and β_u, $D_{\mathrm{loss}}(r_u)$ is the distortion due to channel loss, $P_u(x)$ is the error protection failure rate. The functions $R_{\mathrm{UXP}}(r_u)$ and $P_u(x)$ depend on the error protection scheme used [7].

C. Bit-rate allocation – stationary rate-distortion behavior

In a multi-user video streaming system, clients compete for channel capacity to receive the best video quality. We assume that all users share the same down-link channel and contest for the full range of the channel capacity C.

Assuming that the video R-D relationship is stationary over the duration of the streaming session, the server has to solve the following constrained optimization problem at the beginning of the streaming interval:

$$\begin{aligned} &\min_{\mathbf{r}=[r_1, r_2, ..., r_U]'} \sum_{u=1}^{U} D_u(r_u) \\ &s.t. \sum_{u=1}^{U} R_u(r_u) \leq C, \\ &\mathbf{L} < \mathbf{r} < \mathbf{H}, \end{aligned} \quad (2)$$

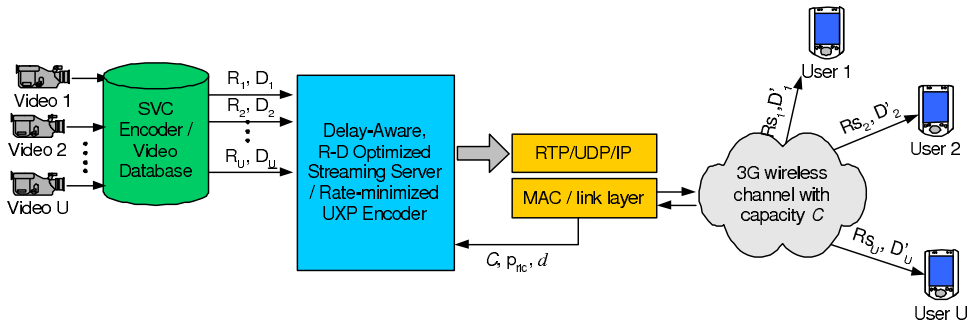

Fig. 2. General structure of the proposed video streaming system over 3G wireless networks. The link layer feeds back the estimated channel capacity C, RLC loss rate p, and the packet delay d to the streaming server. The rate and distortion functions, R_u and D_u, are defined in (1).

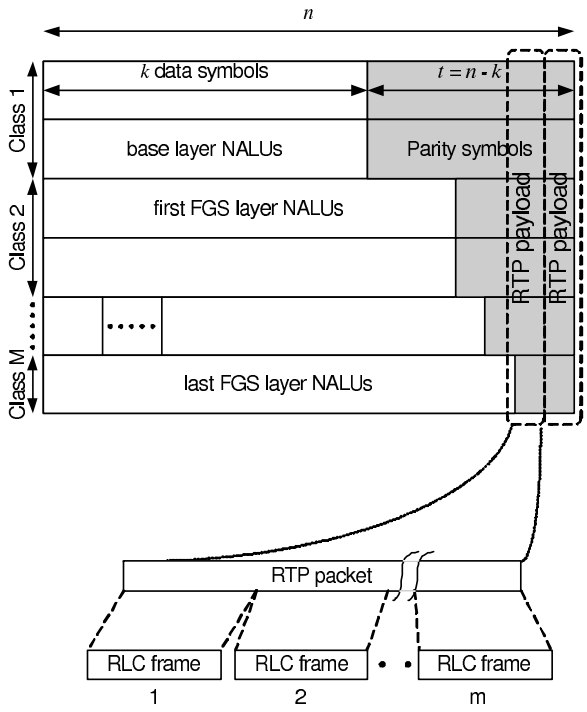

Fig. 3. Standard UXP scheme with FGS layer-based classes. Each RTP packet is also fragmented into m RLC frames. The value of m depends on the link-layer specifications.

where $\mathbf{r}$ is a $(U \times 1)$ vector containing the extracted video bit-rates r_u of user u and bounded below by the base-layer rates $\mathbf{L} = [L_1, ...L_U]'$ and above by the total rates which include all enhancement layers $\mathbf{H} = [H_1, ...H_U]'$.

It is worth noting that the constrained optimization problem defined in (2) satisfies the QoS conditions of delivering a minimum guaranteed video quality for all users. This is established by setting a lower bound L_u on the video extraction rate r_u which corresponds to the base-layer bit-rate of stream u.

III. Packet Delay Restrictions in Video Streaming

In this section, we represent the wireless channel in terms of its variable components and constraints. In what follows, we adopt the protocol stack architecture described in VCEG-N80 [8] for 3GPP network architecture. The video payload is carried over RTP/UDP/IP, where each RTP packet is fragmented into m RLC frames. We assume that the link-layer reports the following fields to the streaming server:

$$\begin{aligned} S_{\text{rlc}} &= \text{the radio-frame size,} \\ p &= \text{steady-state RLC loss rate/probability,} \\ \delta &= \text{queuing delay.} \end{aligned} \tag{3}$$

A. Packet Delay Analysis

Let $\tau_{s,1}$ be the sender time at which the first link-layer frame of an RTP encapsulated NALU is transmitted. The frame is received by the client at time $\tau_{r,1}$ after a delay δ_1, such that

$$\tau_{r,1} = \tau_{s,1} + \delta_1. \tag{4}$$

The second frame is transmitted after one Transmission Time Interval (TTI) at time $\tau_{s,2} = \tau_{s,1} + \xi$ and received at $\tau_{r,2} = \tau_{s,2} + \delta_2$, where ξ is the TTI and $\delta_2 \neq \delta_1$.

In the case where a single NALU is encapsulated in single RTP packet, m RLC frames have to be sent to transmit the NALU, as shown in Figure 4. Let Λ_l be the total delay of NALU l defined as the total time between receiving the first RLC frame and the last frame, and let $\bar{\delta}$ be the average delay for all RLC frames sent and $\tilde{\delta}_i = \delta_i - \bar{\delta}$, then Λ_l is expressed as

$$\Lambda_l = \tau_{r,m} - \tau_{r,1} = (m-1)\xi + \tilde{\delta}_m - \tilde{\delta}_1 \tag{5}$$

The expression for the delay in equation (5) is useful for expressing worst case values for the delay in terms of its mean and standard deviation. Following the analysis in [4], we assume that the packet delay is constrained by the bottleneck link, therefore, the queuing delay can be modeled as a simple M/M/1 queue.

B. UXP Play-out Deadline and Maximum Size

We derive the upper bound on the maximum number of RLC frames allowed per RTP packet of a UXP TB in this subsection. Under UXP, the basic video payload unit is not NALU anymore but the Transmission Block (TB) which contains n RTP packets, each of which is fragmented into m RLC frames. The NALUs of a single GOP are aggregated into one TB in addition to the protection/parity symbols. Moreover,

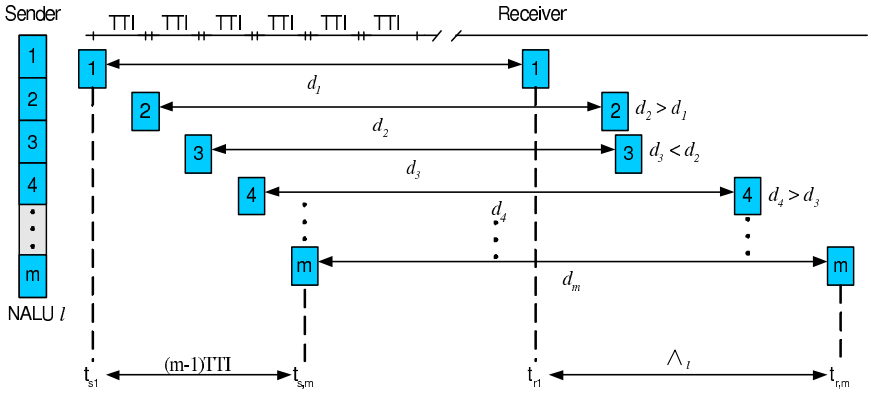

Fig. 4. Timing diagram for the transmission of a NALU indexed by l. The NALU is fragmented into m RLC frames each of which can have a different transmission delay d.

no NALU can be decoded before the entire TB is received at the decoder. Therefore, the new constraint on the number RLC frames per RTP packet of a TB is written as

$$m_t \leq Cm_t = \frac{(t-1)(\frac{N}{f}) - \sum_{i=2}^{t-1}(m_i \times n \times \xi) + \tilde{\delta}_{m_0} - \tilde{\delta}_{m_t}}{n \times \xi}, \tag{6}$$

where m_i is the number of RLC frames per RTP packet in TB i, ξ is the TTI length in seconds, and i is a summation index. We derive this constraint in the remainder of this subsection.

Let t be the TB index in a streaming session, such that $t \in \{0, 1, ..., T\}$, where T is the total number of GOPs in the streaming session. Consider a fixed number of NALUs N per GOP, the play-out deadline of TB 1 can be written as

$$\tau_{DTS,1} = \tau_{m0} + \frac{N}{f}, \tag{7}$$

where τ_{m_0} is the time at which the last RLC frame of TB 0 arrives at the receiver. Following the analysis of Section III, the delay of TB 1 Λ_1 can then be written as

$$\Lambda_1 = \tau_{m1} - \tau_{m0} = n \times m_1 \times \xi + \tilde{\delta}_{m1} - \tilde{\delta}_{m0}, \tag{8}$$

and the general delay constraint equation of TB t is expressed as

$$\Lambda_t \leq (t-1)\frac{N}{f} - \Lambda_{t-1}. \tag{9}$$

We can then extend this analysis to write the constraint Cm_t on the number of RLC frames per RTP packet in TB t as in (6).

Equation (6) above appropriately formulates the delay constraint Cm_t in terms of the delay jitter $\tilde{\delta}$, which is beneficial in the case when the server has statistical knowledge of the channel delay. In such a case, the optimization can be performed for a greedy constraint where the term $\tilde{\delta}_{m0} - \tilde{\delta}_{mt} = -2\sigma$, where σ is the standard deviation of the packet-delay distribution. This worst case scenario arises when the last RLC frame of the first TB 0 arrives one standard deviation σ sooner than the mean delay $\bar{\delta}$, i.e. $\delta_{m_0} = \delta_0 = \bar{\delta} - \sigma$, and the last RLC frame of the current TB l arrives with a delay $\delta_{m_t} = \bar{\delta} + \sigma$.

C. Bit-rate allocation – delay-aware non-stationary behavior

The effect of the play-out deadline of TBs as a result of the RLC frame queuing delays can be included in our constrained optimization setup by forcing additional constraints on the number of allowed RLC frames $m_t^{(u)}$ per RTP packet in TB t of stream u.

The value of $m_t^{(u)}$ is a function of the size of the RTP packet which, in turn, is a function of the size of the TB t. We can express this relationship as follows:

$$m_t^{(u)}(r_u) = \frac{R_{UXP}(r_{u,t}) \times N}{n \times S_{rlc} \times f}.$$

Thus, the modified capacity and delay constrained optimization problem is written as follows:

$$\begin{array}{ll} \min & _{\mathbf{r_t}=[r_{1,t},r_{2,t},...,r_{U,t}]'} \sum_{u=1}^{U} D_u(r_{u,t}) \\ s.t. & \sum_{u=1}^{U} R_u(r_{u,t}) \leq C_t, \\ and & m_t^{(u)} \leq Cm_t^{(u)}, \text{ where } u \in \{1, 2, ...U\}, \end{array} \tag{10}$$

Cm_t is defined in (6).

IV. On the non-convexity of the Rate Allocation Problem

In this section, we study the nature of the constrained optimization problems described above in terms of convexity and complexity of solution. The constrained optimization problems described above can be generalized in terms of the following problem:

$$\begin{array}{ll} \min & _{\mathbf{x}=[x_1,x_2,...,x_U]'} \sum_{u=1}^{U} D_u(x_u) \\ s.t. & \sum_{u=1}^{U} R_u(x_u) \leq C, \\ and & m_u(x_u) \leq Cm_u, \text{ for all } u \in \{1, 2, ...U\}. \end{array} \tag{11}$$

Equations (12) and (13) list the components of each of the objective and constraint functions as well as their relation to the terms previously defined in this paper.

Objective:

$$\begin{array}{lcl} D_u(x_u) & = & d_u(x_u) - \int_{L_u}^{x_u} p_u(s) d'_u(s) ds, \\ d_u(x_u) & = & \alpha_u + \frac{\theta_u}{x_u - \beta_u}, \\ P_u(x_u) & = & \text{increasing piecewise constant function} \\ & & \text{of } x_u \text{ with range } [0, 1]. \end{array} \tag{12}$$

Constraints:

$$\begin{array}{lcl} R_u(x_u) & = & (1+a)\int_{L_u}^{x_u} h_u(s)ds \\ m_u(x_u) & = & b\int_{L_u}^{x_u} h_u(s)ds, \\ h_u(x_u) & = & \frac{n}{k_u(x_u)} \\ & = & \text{decreasing piecewise constant function} \\ & & \text{of } x_u \text{ with range } [1,2], \end{array} \tag{13}$$

where a and b are positive constants $\ll 1$.

Since $d_u(x_u)$ is, by definition, a monotonically decreasing convex function of x_u over the interval $L_u \leq x_u \leq H_u$, with $d'_u(x_u) < 0$ and $d''_u(x_u) > 0$, the first and second derivatives of $f_u(x_u)$ are shown below:

$$\begin{array}{ll} f'_u(x_u) & = (1-p_u(x_u))d'_u(x_u) \leq 0 \\ f''_u(x_u) & = (1-p_u(x_u))d''_u(x_u) - p'_u(x_u)d'_u(x_u) \geq 0 \end{array} \tag{14}$$

with equality at $p_u(x_u) = 1$. Thus, the objective function $f_u(x_u)$ is only once differentiable, piecewise convex.

The constraint functions $R_u(x_u)$ and $m_u(x_u)$, on the other hand, which are scaled versions of the same function $e_u(x_u)$ shown in (15) below, are concave piecewise linear.

$$\begin{array}{ll} e_u(x_u) & = \int_{L_u}^{x_u} h_u(s)ds \\ e'_u(x_u) & = h_u(x_u) > 0 \\ e''_u(x_u) & = h'_u(x_u) \leq 0. \end{array} \tag{15}$$

As a result, we are faced with a non-convex, non-differentiable optimization problem. One method of solving this nonconvex problem is to use augmented Lagrangian algorithms [9]. We refer the reader to [9] for proof of convergence.

V. Simulations and Results

In this section, we study the performance of the different rate-allocation schemes formulated in Sections II-C and III-C. For our performance testing, we encoded and prioritized 9 video sequences: Bus, Foreman, Crew, Mobile, Harbor, City, Football, Ice, and Soccer in CIF resolution at 15 frames per second in SVC using JSVM6 available from [10]. The encoded streams are composed of an H.264/AVC compatible base layer and 2 FGS enhancement layers.

A. Scheme definition

We define three streaming schemes differing in UXP allocation and the rate extraction:

Optimized UXP, fixed rate (OUFR): The UXP encoder uses the optimized UXP approach described in [7] to allocate the R-S parity symbols. Rate extraction is performed by dividing the bit-rate range $[L_u, H_u]$ of each video stream into 1000 steps and then incrementing the base-layer rate L_u by one step-size for each user until the capacity constraint is satisfied. No consideration is given to the delay constraint or fluctuation of video bit-rate over the duration of the streaming session.

Optimized UXP, optimized rate (OUOR): In this scheme we use the optimized UXP approach and the time-averaged rate allocation scheme described in Section II-C. Delay constraints and video bit-rate fluctuation are not considered.

Delay-aware multi-interval optimized UXP, optimized rate (DMOUOR): The UXP encoder performs optimal UXP allocation at each interval t using an estimated $p_{rtp,t}$ value. The video bit-rate fluctuation is taken into consideration, and a multi-interval rate allocation with delay constraints is performed in the rate-allocation procedure for each of the T intervals as described in Section III-C.

B. Performance Testing

We simulate the lossy channel using the 3GPP off-line simulator available from [11], listed in [12]. Moreover, we have added a UXP encoder and decoder to simulate the specifications listed in [6]. The UXP encoder aggregates all NALUs (base-layer and FGS) belonging to a single GOP into one TB and encapsulates each column of the TB in a single RTP packet according to [13]. We have performed several modifications to the software in [11] in order to add the effect of packet delay and channel capacity on the streaming system. In the case of packet delay, the 3GPP simulator drops all RTP packets belonging to a TB that exceed the play-out deadline of the TB.

We simulate link-layer frame loss rates of 1%, 3%, and 10% as provided by the first three radio bearer bit-error traces in [11]. We also consider channel capacities of 3.6Mbps, 5.3Mbps, 7.2Mbps, and 10.7Mbps. As a performance metric, we use the average PSNR of all 9 streams given by:

$$PSNR = 10\log_{10}\left[\frac{(255)^2}{\sum_{u=1}^{9} MSE_u/9}\right],$$

where MSE_u is the luminance mean square error of user u.

Figures 5 (a) and (b) compare the performance of each of the three schemes OUFR, OUOR, and DMOUOR for a play-out deadline of 533 ms with varying capacities and varying PLRs, respectively. Both figures show that DMOUOR achieves significant gains over the other schemes with maximum gains of 2dB for the 10% loss rate and 10.7 Mbps capacity (Figure 5 (a)) and 1.65dB for 10% PLR and 3.6Mbps capacity (Figure 5 (b)). The performance gains exhibited by the delay-aware DMOUOR scheme as shown in Figure 5 emphasize the importance of delay-aware rate allocation in video streaming. For OUFR, the increase in capacity, which translates into looser delay constraints, results in embedding more FGS enhancement packets. However, this results in an overabundance of enhancement layer RLC frames which replace base layer packet transmissions resulting in poorer quality. The smarter rate-allocation used in the OUOR scheme results in a relatively better performance than OUFR, however, it is no match for the delay-aware DMOUOR scheme.

Next, we compare the performance of the DMOUOR, OUOR, and OUFR schemes under different delay constraints. Figure 6 demonstrates the improved performance of DMOUOR over the other schemes for different values of the video play-out deadline. The tests are performed for play-out deadlines of 266, 400, 533, 666, and 800 msec with a 5.3 Mbps channel capacity and 3% packet loss rate. The figure shows that the improvement of DMOUOR is more significant for tighter delay constraints.

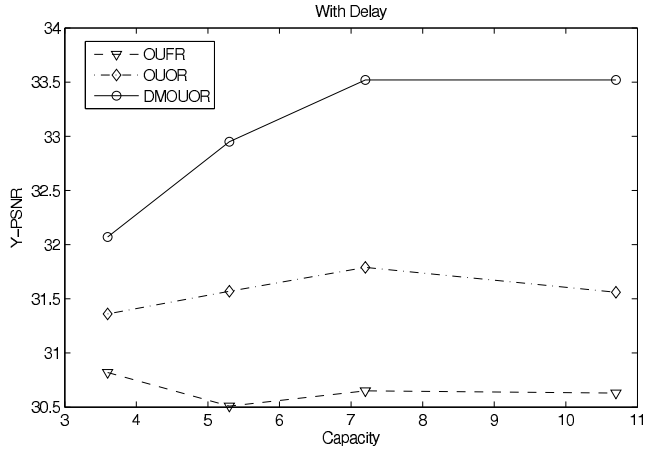

(a) Y-PSNR vs channel capacity

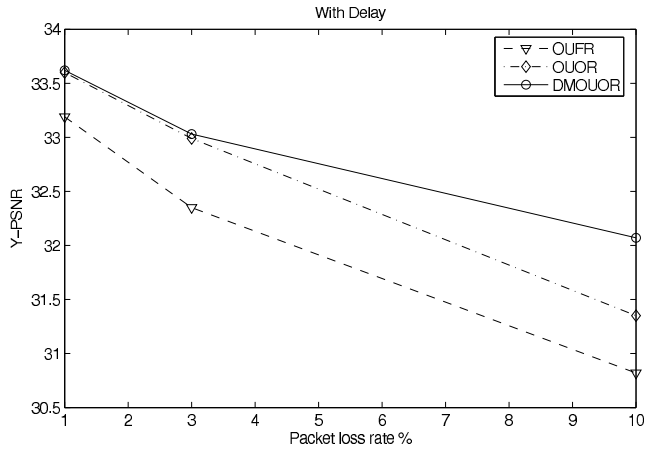

(b) Y-PSNR vs RLC packet loss rate

Fig. 5. Comparison of the Y-MSE performance between the three streaming schemes OUFR, OUOR, and DMOUOR with the effect of packet delay as described in Section III-C.

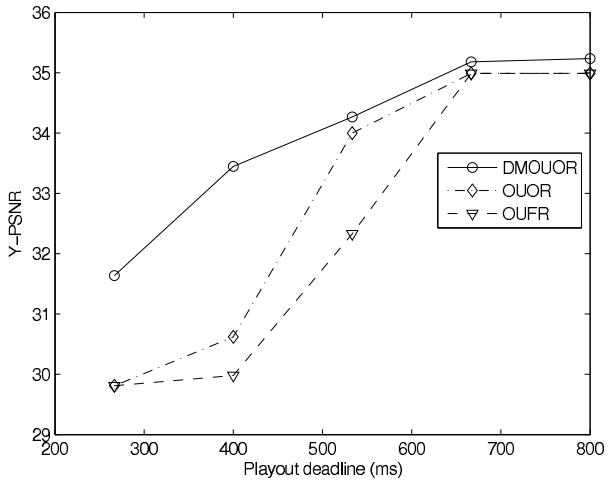

Fig. 6. Comparison of the Y-PSNR performance between the three schemes DMOUOR, OUOR, and OUFR for different play-out deadlines over a channel with 5.3 Mbps capacity and 3% PLR.

VI. Conclusion

We have analyzed the performance of five multi-user scalable video streaming strategies in a simulated wireless network scenario which suffers from limited capacity and packet loss. For our analysis, we derived an analytical expression for the delay and play-out deadlines for UXP protected video streams and incorporated this expression in a delay-aware rate-constrained streaming scheme (DMOUOR). Finally, the performance gains of 1.65dB to 2dB in Y-PSNR demonstrated by our delay-aware DMOUOR scheme compared to delay un-ware schemes come at the cost of increased *off-line* computational complexity which does not affect the run-time performance of the streaming system.

References

[1] M. V. D. Schaar and S. Shankar, "Cross-Layer Wireless Multimedia Transmission: Challenges, Principles, and New Paradigms," *IEEE Wireless Communications Magazine*, vol. 12, no. 4, pp. 50–58, August 2005.

[2] P. Pahalawatta, R. Berry, T. Pappas, and A. Katsaggelos, "Content-Aware Resource Allocation and Packet Scheduling For Video Transmission Over Wireless Networks," *IEEE Journal on Selected Areas in Communications, Special Issue on Cross-Layer Optimization for Wireless Multimedia Communications*, vol. 25, pp. 749–759, May 2007.

[3] P. A. Chou and Z. Miao, "Rate-Distortion Optimized Streaming of Packetized Media," Microsoft Corporation, Technical Report MSR-TR-2001-35, February 2001.

[4] X. Zhu, P. Agrawal, J. P. Singh, T. Alpcan, and B. Girod, "Rate Allocation for Multi-User Video Streaming over Heterogenous Access Networks," in *ACM Multimedia*, September 2007.

[5] G. Liebl, M. Wagner, J. Pandel, and W. Weng, "An RTP Payload Format for Erasure-Resilient Transmission of Progressive Multimedia Streams," IETF, October 2004.

[6] T. Schierl, H. Schwarz, D. Marpe, and T. Wiegand, "Wireless Broadcasting Using The Scalable Extension of H.264/AVC," in *IEEE International Conference on Multimedia and Expo (ICME)*, July 2005.

[7] H. Mansour, V. Krishnamurthy, and P. Nasiopoulos, "Channel Adaptive Multi-User Scalable Video Streaming with Unequal Erasure Protection," in *International Workshop on Image Analysis and Multimedia Interactive Services (WIAMIS 2007)*, June 2007, pp. 54–57.

[8] V. Varsa, M. Karczewicz, G. Roth, R. Sjberg, T. Stockhammer, and G. Liebl, *Common Test Conditions for RTP/IP over 3GPP/3GPP2* , ITU-T SG16 Q6 Video Coding Experts Group (VCEG), December 2001.

[9] D. P. Bertsekas, *Nonlinear Programming*. Belmont, MA: Athena Scientific, 1999.

[10] ISO/IEC JTC 1/SC 29/WG 11 N8752, "JSVM-6 software," 2006. [Online]. Available: http://mpeg.nist.gov/reg/_listwg11_76.php

[11] "3GPP/3GPP2 Offline Simulator S4-040803." [Online]. Available: http://www.3gpp.org/ftp/tsg_sa/WG4_CODEC/TSGS4_33/Docs/S4-040803.zip

[12] Y. K. Wang, S. Wenger, and M. M. Hannuksela, *Common conditions for SVC error resilience testing*, Joint Video Team (JVT) of ISO/IEC MPEG and ITU-T VCEG JVT-P206d1, July 2005.

[13] S. Wenger, M. Hannuksela, T. Stockhammer, M.Westerlund, and D. Singer, *RTP Payload Format for H.264 Video*, IETF RFC3984, February 2005.